

Preliminary Plan of Numerical Simulations of Three Dimensional Flow-Field in Street Canyons

Liang Zhiyong, Zhang Genbao and Chen Weiya
*College of Science Donghua University
China*

1. Introduction

Along with the rapid development of urban construction, the rapid increase the number of motor vehicles, so that the city's air pollution worsened in some areas of serious deterioration in air quality. With the increased concern over pollutants in urbanized cities, extensive investigation such as field measurements, laboratory-scale physical modelling and computational fluid dynamics techniques (CFD), have been launched in recent years to study the wind flow in street canyons^[1]. The major parameters affecting pollutant transport are ambient conditions(wind speed and direction), building geometry(height, width, and roof shape), street dimensions(width), model of dimensions etc, and these factors should be considered. But with the limit of computational techniques, based on the three-dimensional numerical simulation is not widely carried out, particularly for some of the complex structure of the street (as a crossroads) study of literature is more rare, most studies(e.g., Kim and Baik (2001), Chan et al.(2002)) employ high-quality two-dimensional numerical simulations approach^[2]. However, with the ever-increasing computational power, it is now feasible to employ three-dimensional numerical simulations technique to simulate building-scale flow and dispersion in real street canyons.

2. Computational model and boundary conditions

2.1 Computational model

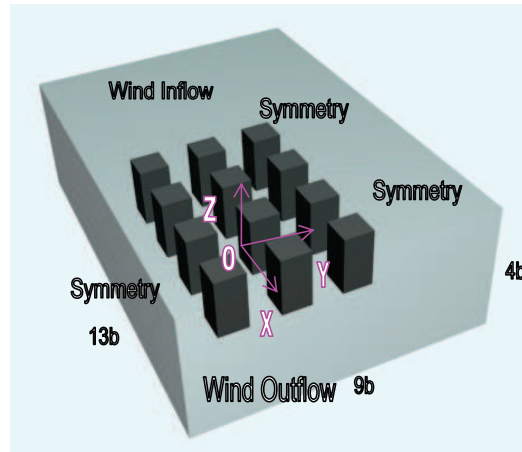
The three-dimensional computational domain consists of two parallel arranged in a string of street in the streamwise direction. The origin of coordinates is located in the center of the bottom of the buildings. (Fig.1). The flow properties of the street canyon of the domain are presented in the following discussion. h and b denotes the height and the width of the street canyon, respectively. The height of the street canyon of aspect ratio ($H=h=2b$) and the free-stream inflow speed U are considered as the reference length and velocity scales, respectively. The Reynolds number is prescribed at 9.0×10^5 . The flow is treated as an incompressible, isothermal, and pseudo steady-state turbulence^[2].

2.2 Boundary conditions

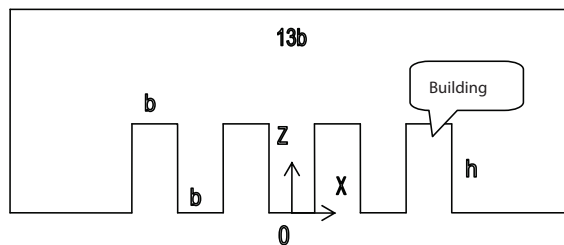
In the three-dimensional computational domain, the solid boundaries at the bottom and around the building are assumed as no-slip wall conditions. The inlet boundary condition in

the upstream direction: $u = U, v = 0, \omega = 0$. The outlet boundary condition in the downstream direction: $\frac{\partial u}{\partial x} = 0, \frac{\partial v}{\partial y} = 0, \frac{\partial \omega}{\partial z} = 0$. Other boundaries are considered as symmetry conditions: $u = U, v = 0, \omega = 0$. (Fig.1)

3. Figures



(a) Stereogram



(b) Projection of X-Y plane

Fig. 1. Computational model and Boundary conditions

4. Equations

In the use of software "Fluent" to model calculation, the first step needs to build a variety of Street Canyon models and a reasonable mesh in pre-processor Gambit, and then the definition of the boundary conditions and the physical model can be used to solve the model in fluent software.^[3]

The three-dimensional computational domain chooses hex and wedge grids. The total numbers of the grids is 2,755,206. The precision ϵ takes 10^{-6} . This simulation carries on by the parallel computer in Donghua University. The coming velocity: $U = 2.0 \text{ m/s}$.

In this paper the results are based on the numerical solution to the governing fluid flow and transport equations, which are derived from basic conservation principles as follows:

The mass conservation equation^[4]:

$$\frac{\partial \bar{u}_i}{\partial x_i} = 0 \tag{1}$$

(\bar{u}_i mean velocity component in the (x, y, z) directions (ms^{-1}))

The momentum conservation (Navier-Stokes) equation^[4]:

$$u_j \frac{\partial \bar{u}_i}{\partial x_j} = \left(\frac{\rho - \rho_n}{\rho_n}\right)g_i - \frac{1}{\rho} \frac{\partial \bar{p}}{\partial x_i} + \frac{\partial}{\partial x_j} \left(\nu \frac{\partial \bar{u}_i}{\partial x_j} - \bar{u}_i \bar{u}_j'' \right) \tag{2}$$

(\bar{u}_i mean velocity component in the (x, y, z) directions (ms^{-1}); \bar{u}_i'' mean velocity fluctuation in the (x, y, z) directions (ms^{-1}); ν mean kinematic viscosity (ms^{-1});

g mean acceleration due to gravity (ms^{-2}))

The realizable $k - \epsilon$ equations^[4]:

$$\bar{u}_i \frac{\partial k}{\partial x_i} = \frac{1}{\rho} \frac{\partial}{\partial x_i} \left[\left(\mu + \frac{\mu_t}{\sigma_k} \right) \frac{\partial k}{\partial x_i} \right] + \frac{1}{\rho} P_k - \epsilon + \frac{1}{\rho} G_b \tag{3}$$

$$\bar{u}_i \frac{\partial \epsilon}{\partial x_i} = \frac{1}{\rho} \frac{\partial}{\partial x_i} \left[\left(\mu + \frac{\mu_t}{\sigma_k} \right) \frac{\partial \epsilon}{\partial x_i} \right] + C_1 S_\epsilon - C_2 \frac{\epsilon^2}{k + \sqrt{\nu \epsilon}} + \frac{1}{\rho} C_{\epsilon 1} \frac{\epsilon}{k} C_{\epsilon 3} G_b \tag{4}$$

($G_b = \beta g \frac{\mu_t}{Pr_t} \frac{\partial \bar{\theta}}{\partial x_i}$; $\mu_t = \rho C_\mu \frac{k^2}{\epsilon}$; $P_k = \nu_t \times \frac{\partial \bar{u}_i}{\partial x_j} \left(\frac{\partial \bar{u}_i}{\partial x_j} + \frac{\partial \bar{u}_j}{\partial x_i} \right)$; $\sigma_k = 1.0$; $C_{\epsilon 1} = 1.44$; $C_{\epsilon 3} = \tanh |v/u|$;

β mean the thermal expansion coefficient)

5. Conclusion

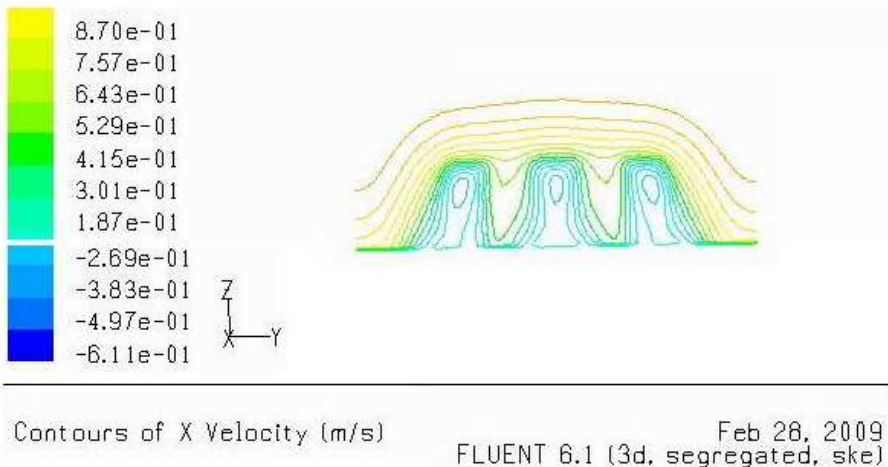


Fig. 2. Velocity distribution in y-z plane at $x = 0.0$ and a Reynolds number is 9.0×10^5

Fig. 2 depicts clearly a large vorticity in the back of the buildings in the direction of the wind. More detailed analysis reveals that some of the second vorticity, which are recent Oval, can be clearly observed in the back of the buildings. In addition, flow lines are basically as the same as the profile of the streets.

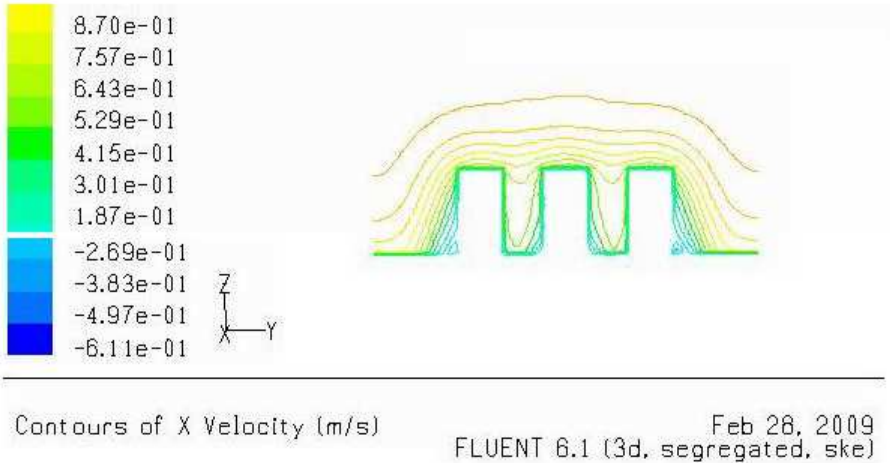


Fig. 3. Velocity distribution in y-z plane at $x = 1.0$ and a Reynolds number is 9.0×10^5

Fig. 3 shows that in a cross-section of the building, none of vorticity can be found in the streets, but a small vorticity is observed in the bottom of the both sides of buildings. In addition, flow lines are basically as the same as the profile of the streets.

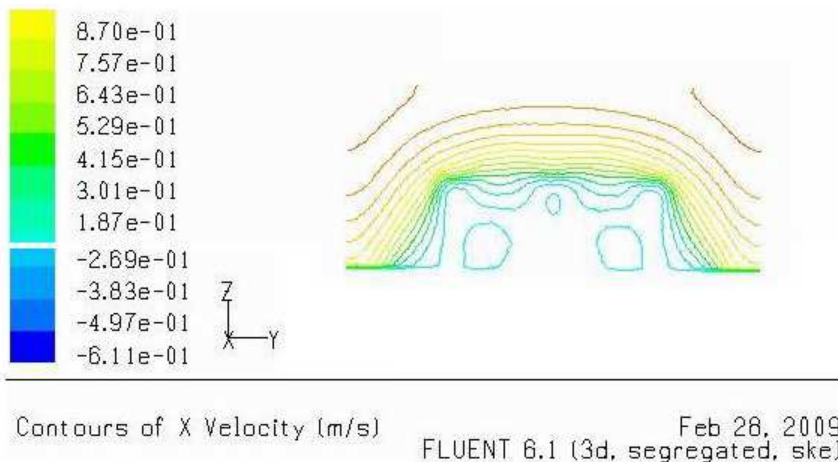


Fig. 4. Velocity distribution in y-z plane at $x = 2.0$ and a Reynolds number is 9.0×10^5

Fig. 4 depicts clearly some recent circle vorticities in the back of the buildings in the direction of the wind. In the back of the buildings of both sides, a large vorticity is found and in the middle of the back of the building, a vorticity is observed at the top of the streets. In addition, flow lines are basically as the same as the profile of the streets.

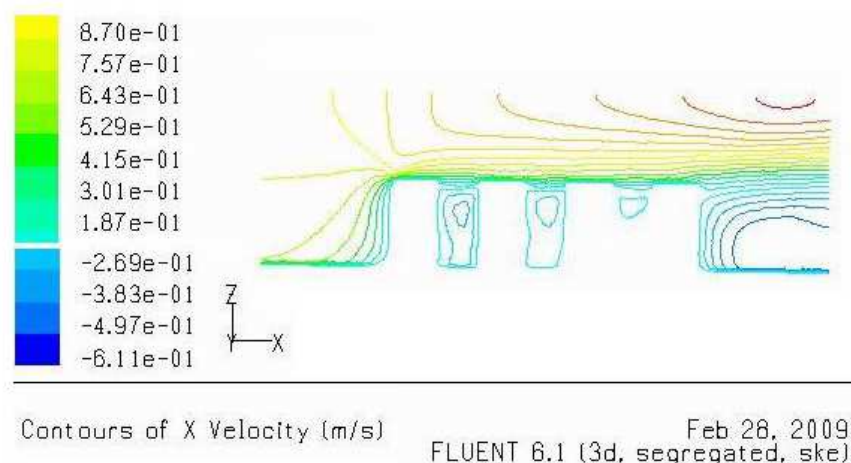


Fig. 5. Velocity distribution in x-z plane at $y = 0.0$ and a Reynolds number is 9.0×10^5

As shown in Fig. 5, some strong vorticities are found in the every target streets. The flow lines are raised when it first reaches the urban building. The flow lines at roof level are almost parallel to the ground after the flow passed several urban buildings with identical height. The flow under this configuration is found to be stable within the whole simulation period, as also stated by Gerdes and Olivari (1999).^[5]

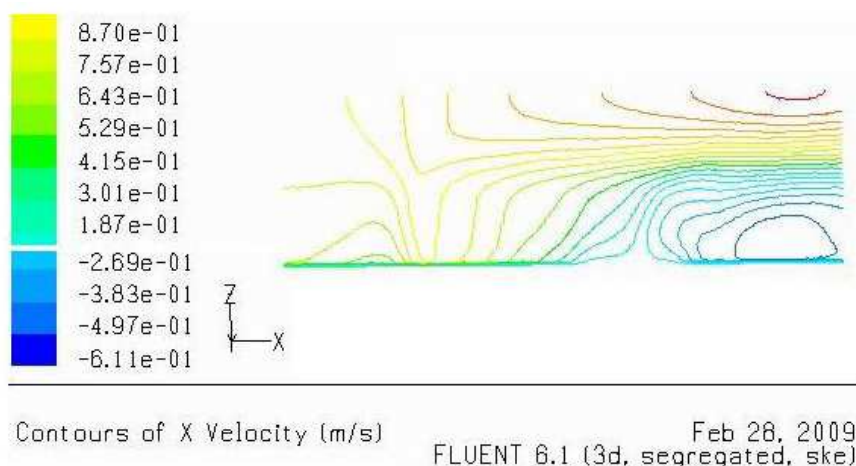


Fig. 6. Velocity distribution in x-z plane at $y = 1.0$ and a Reynolds number is 9.0×10^5

As shown in Fig. 6, there is no vorticity, in the direction of the wind, the speed lines are sparse, while the flow lines are intensive in the leeward direction, The flow lines at roof level is almost parallel to the ground after the flow passed several urban buildings with identical height.

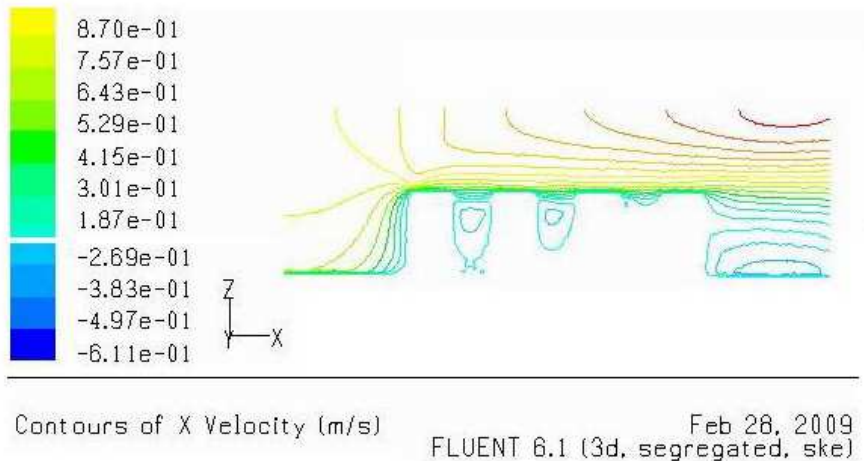


Fig. 7. Velocity distribution in x-z plane at $y = 2.0$ and a Reynolds number is 9.0×10^5

As shown in Fig. 7, some strong vorticities are found in the every target streets. The first street in the direction of wind has a large vorticity, in the first two streets, there are respectively two vorticities (a large vorticity, a small vorticity), and the vorticity can not be found in the last street. But some vorticities can be found on the lower part of the building in the leeward direction at the bottom of the streets.

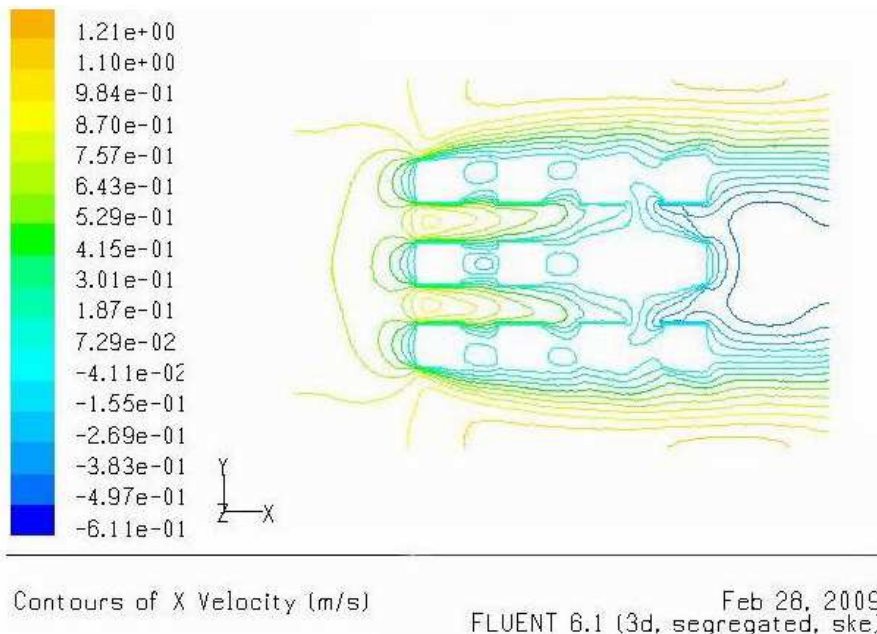


Fig. 8. Velocity distribution in x-y plane at $z = 0.5$ and a Reynolds number is 9.0×10^5

As described in Fig. 8, some strong vorticities are found in the every target streets. The number of vorticity in the direction of the wind is more than that in the leeward direction. some large recent oval vorticity can be found in the back of the buildings in the direction of the wind. It is found that the wind is difficult to go through the streets.

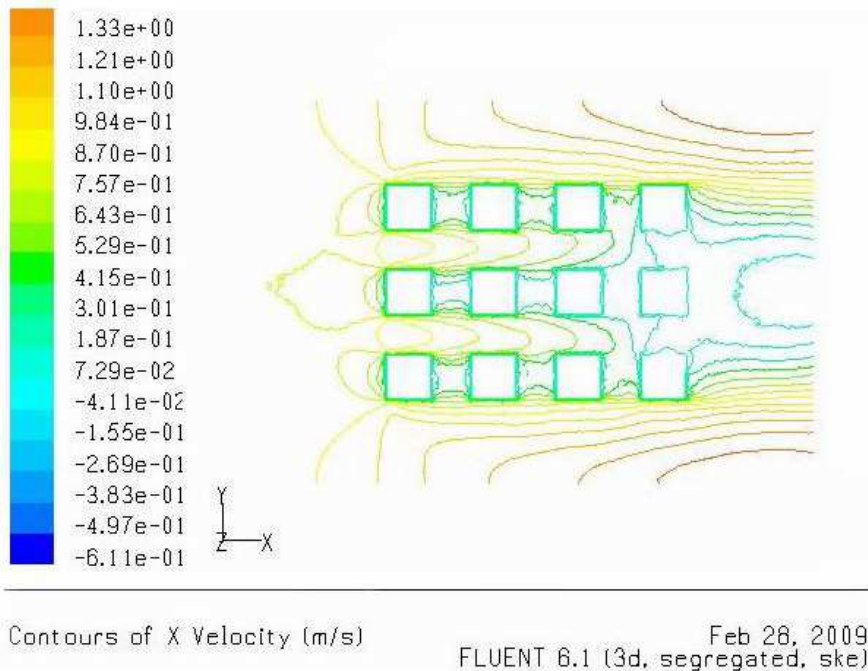


Fig. 9. Velocity distribution in x-y plane at $z = 2.0$ and a Reynolds number is 9.0×10^5

As described in Fig. 9, some strong vorticities are found in the every target streets. With the high degree increasing, there is a clear vorticity on the back part of the building in the leeward direction. In addition, flow lines are basically as the same as the profile of the streets.

As described in Fig. 10, none of strong vorticity is found on this cross-section. The contours of x velocities are not found above the streets, so the flow of this part, to the basic, is unchanged.

Three-dimensional flow-field is investigated in street canyons at a Reynolds number of 9.0×10^5 using a realizable $k - \varepsilon$ model, and we get the results (depicted in the front). The present model can exactly describe the flow-field in street canyons and we can get the results in any directions. The results of the present numerical model show that X velocity in the upstream directions is as same as that outside the street canyon, but X velocity is lower in most parts of inside the street canyons, and the air inside and outside streets is difficult to be exchanged. In this paper only the velocities in X direction could be shown, other results are not mentioned. The pollution in the streets does not considered. So, More works need to be done to perfect our research.

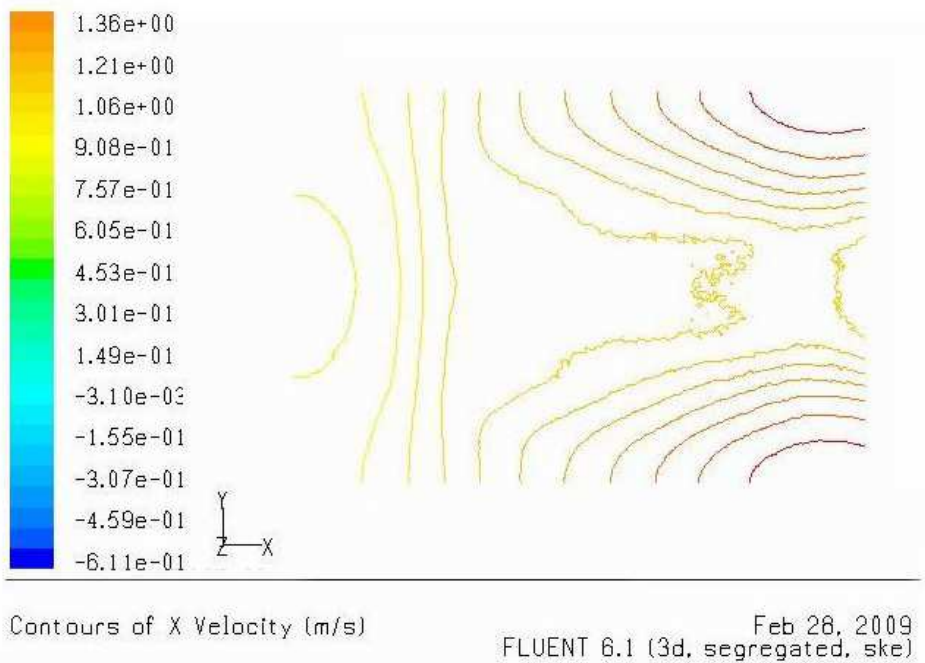
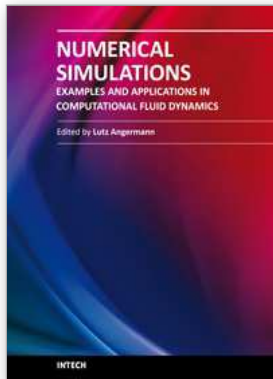


Fig. 10. Velocity distribution in x-y plane at $z = 3.0$ and a Reynolds number is 9.0×10^5

6. References

- [1] Recent progress in CFD modelling of wind field and pollutant transport in street canyons, Xian-Xiang Li^a, Chun-Ho Liu^b, Dennis Y.C. Leung^a, K.M. Lam^c, Atmospheric Environment 40 (2006) 5640-5658
- [2] Development of a $k-\varepsilon$ model for the determination of air exchange rates for street canyons, Xian-Xiang Li, Chun-Ho Liu, Dennis Y.C. Leung, Atmospheric Environment 39 (2005) 7285-7296, Atmospheric Environment 40 (2006) 5640-5658
- [3] Pollutant dispersion in urban street canopies, Jiyang Xia, Dennis Y.C. Leung, Atmospheric Environment 35 (2001) 2033-2043
- [4] Computational Fluid Dynamics The Basics with Applications, John D. Anderson, JR, 1995 by McGraw-Hill Companies, Inc.
- [5] On the prediction of air and pollutant exchange rates in street canyons of different aspect ratios using large-eddy simulation, Chun-Ho Liu^a, Dennis Y.C. Leung^a, Mary C. Barth^b, Atmospheric Environment 39 (2005) 1567-1574.



Numerical Simulations - Examples and Applications in Computational Fluid Dynamics

Edited by Prof. Lutz Angermann

ISBN 978-953-307-153-4

Hard cover, 440 pages

Publisher InTech

Published online 30, November, 2010

Published in print edition November, 2010

This book will interest researchers, scientists, engineers and graduate students in many disciplines, who make use of mathematical modeling and computer simulation. Although it represents only a small sample of the research activity on numerical simulations, the book will certainly serve as a valuable tool for researchers interested in getting involved in this multidisciplinary field. It will be useful to encourage further experimental and theoretical researches in the above mentioned areas of numerical simulation.

How to reference

In order to correctly reference this scholarly work, feel free to copy and paste the following:

Genbao Zhang, Weiya Chen and Zhiyong Liang (2010). Preliminary Plan of Numerical Simulations of Three Dimensional Flow-Field in Street Canyons, Numerical Simulations - Examples and Applications in Computational Fluid Dynamics, Prof. Lutz Angermann (Ed.), ISBN: 978-953-307-153-4, InTech, Available from: <http://www.intechopen.com/books/numerical-simulations-examples-and-applications-in-computational-fluid-dynamics/preliminary-plan-of-numerical-simulations-of-three-dimensional-flow-field-in-street-canyons>

INTECH

open science | open minds

InTech Europe

University Campus STeP Ri
Slavka Krautzeka 83/A
51000 Rijeka, Croatia
Phone: +385 (51) 770 447
Fax: +385 (51) 686 166
www.intechopen.com

InTech China

Unit 405, Office Block, Hotel Equatorial Shanghai
No.65, Yan An Road (West), Shanghai, 200040, China
中国上海市延安西路65号上海国际贵都大饭店办公楼405单元
Phone: +86-21-62489820
Fax: +86-21-62489821

© 2010 The Author(s). Licensee IntechOpen. This chapter is distributed under the terms of the [Creative Commons Attribution-NonCommercial-ShareAlike-3.0 License](#), which permits use, distribution and reproduction for non-commercial purposes, provided the original is properly cited and derivative works building on this content are distributed under the same license.